Int. J. Electrochem. Sci., 12 **(2017)** 7853 – 7868, doi: 10.20964/2017.08.33

International Journal of
ELECTROCHEMICAL
SCIENCE
www.electrochemsci.org

Effect of Traces of Dissolved Oxygen on the Passivation Stability of Super 13Cr Stainless Steel Under High CO_2/H_2S Conditions

Xiaoqi Yue[1], *Lei Zhang*[1,*], *Dapeng Li*[2], *Hiroshi Honda*[1], *Minxu Lu*[1], *Zhu Wang*[1], *Xian Tang*[1]

[1] Institute of Advanced Materials and Technology, University of Science and Technology Beijing, Beijing, 100083, P. R. China.
[2] Safetech Research Institute, Beijing, 100083, P. R. China.
[*]E-mail: zhanglei@ustb.edu.cn

Received: 29 March 2017 / *Accepted:* 31 May 2017 / *Published:* 12 July 2017

Despite being widely used under a variety of oxygen-free conditions, super 13Cr stainless steel (13% Cr) may suffer serious failure in the presence of traces of oxygen. However, very little attention has been paid to the effect of traces of dissolved oxygen (DO, ppb levels) on the corrosion resistance of stainless steels. We used the potential of electrochemical characterization techniques (e.g., cyclic polarization and surface analysis) to study the effect of traces of DO (10–1000 ppb) on the stability of the passive film generated on super 13Cr stainless steel under high CO_2/H_2S conditions (typical of oil and gas production). DO was demonstrated to accelerate both the anodic and cathodic processes. The sensitive DO levels at varying conditions were determined by conducting electrochemical experiments under different concentrations of DO. The results showed that the passive current density increased with the concentration of DO in CO_2/H_2S solutions. The stability of the passive film decreased with the concentration of DO.

Keywords: super 13Cr; oxygen corrosion; critical dissolved oxygen levels; passive film.

1. INTRODUCTION

Super 13Cr, a martensite stainless steel, is widely used under oxygen-free working conditions in the chemical, oil, gas, and nuclear power industries owing to its high strength and corrosion resistance resulting from the Cr_2O_3 passivation film formed upon addition of 12–14% Cr [1,2]. However, the limitations of super 13Cr for some applications still remain unsolved because of the complex interaction of several environmental factors [3]. Since downhole tubing typically operates under oxygen-free conditions, the metal surface corrosion process is mainly governed by reduction

reactions (i.e., hydrogen evolution reaction, HER) [4]. However, this metal surface corrosion reaction is affected by the presence of dissolved oxygen (DO) even at low levels [5]. While originally unpassivated, carbon steels can build up surface passivation films in the presence of low levels of DO [6–8]. However, in the case of stainless steels having self-passivation abilities, low levels of DO can change the passivation properties of these materials, thereby altering their corrosion resistance [9].

The oxygen content has been recently found to greatly alter the surface passivation films of stainless steels in sodium chloride brine solutions. The stability of the surface passivation films of different kinds of stainless steels was found to differ in aerated and deaerated Cl^- solutions (100,000 ppm) [10]. According to previous studies, this influence of DO mainly resulted from changes in the cathodic and anodic processes [11]. Since the active–passive–transpassive transition is mainly affected by the cathode process in weak acid solutions, high DO levels can even result in the disappearance of the passivation characteristics of stainless steels when submerged in borated and lithiated waters at low pH and high temperature [12]. However, according to some studies, a dissolved passivating oxidizer such as DO only provides the required potential for passivation without introducing any additional chemical species involved in the passivation process [13]. Even 10 ppb of DO were found to increase the corrosion potential of stainless steels at high temperatures by altering the outer oxide film products [14–16]. Thus, the poorer corrosion resistant performance of these materials is thought to originate from variations in the surface passive film [17]. Under sweet conditions, both CO_2 and O_2 were found to alter the surface passivation characteristics of stainless steels, although the effect of DO was significantly more pronounced [18]. Thus, traces of oxygen (i.e., 50 ppb) produced higher effects on the surface passivation stability of duplex and super duplex stainless steels than 2 bar of CO_2 [19]. Moreover, under sour conditions, the effects of H_2S and other sulfur compounds on stainless steels are generally ascribed to the adsorption of sulfur atoms (S_{ads}) on the alloy surface, which is covered by oxygen atoms [20]. The damage of the surface passivation film of stainless steels might result in the formation of cracks. It was also found that the combined action of DO and chloride in water significantly accelerated the stress corrosion cracking (SCC) growth rates in stainless steels [21]. Apparently, DO was actively involved in accelerating crack propagation processes, thereby reducing the fatigue strength [22,23].

Since DO is widely accepted as a key factor controlling the stability of the surface passivation films of stainless steels, this parameter is currently monitored while evaluating the corrosion resistant performance of these materials [24]. However, the DO content significantly fluctuates within a small range depending on environmental and process characteristics. Accurate control of the DO content during an experimental process has not been achieved yet. According to the standards revised in 2016 (i.e., laboratory testing of metals for resistance to sulfide stress cracking and stress corrosion cracking in H_2S environments - NACE TM 0177-2016), the maximum allowable DO content is 50 ppb [25]. According to previous research results, the type of material, the temperature, the pH value, and the corrosion medium alter the effect of DO on the surface passivation properties of stainless steels. Thus, it is difficult to determine the influence of DO exclusively. This paper studied the impact of low levels (10–1000 ppb) of DO on the surface passivation properties of a super 13Cr stainless steel in CO_2/H_2S sodium chloride solutions. Thus, the sensitive levels of DO under CO_2/H_2S conditions were studied as a guide for applying super 13Cr stainless steel under oxygen-free or low DO-level environments.

Additionally, this work was aimed to provide support to the later studies on maximal DO levels for various kinds of stainless steel under working conditions.

2. EXPERIMENTAL

The chemical composition and microstructure characteristics of the super 13Cr martensitic stainless steel used herein are shown in Table 1 and Figure 1, respectively. This material belongs to the low-carbon (< 0.03%), low-alloy (Mo) 0.95%, 13% Cr steel family. This material showed a homogenous microstructure, with austenite being present in residual amounts and martensite showing tiny acicular and twin substructures.

Table 1. Chemical composition of super 13Cr (wt%).

Stainless Steel	Chemical compositions (wt%)							
	C	Si	Mn	P	S	Cr	Ni	Mo
super 13Cr	0.027	0.16	0.37	0.013	0.0026	12.82	3.95	0.95

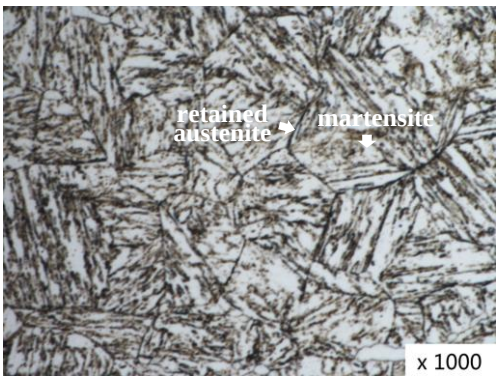

Figure 1. Microstructure of the super 13Cr stainless steel used herein.

All samples (10 mm × 10 mm × 3 mm in size) were mounted in a plastic tube and sealed with an epoxy resin. Before each experiment, the working surface of the specimen was abraded (mirror finish) with a 2000 SiC paper, rinsed in distilled water and acetone, and finally dried under cool air. The electrochemical experiments were carried out under ambient pressure in organic glass cells independently designed with a saturated calomel electrode (SCE) serving as the reference electrode. High temperature and high pressure (HTHP) electrochemical experiments were carried out in an autoclave with Ag/AgCl as the reference electrode. All experiments described herein employed platinum as the counter electrode. The cyclic voltammetry curves were determined upon scanning the potential (scanning rate: 0.5 mV/s) from -100 to 2500 mV (vs state open circuit potential (E_{ocp})).

Since the rate of water formation usually increases with the depth and the temperature under oil and gas conditions, the 5 wt% NaCl solution can be considered a typical ambient-temperature condition, while a 9.5 wt% NaCl solution is likely to be found under HTHP conditions. Based on the

above, 5 and 9.7 wt% NaCl solutions were selected as test solutions. These solutions were previously deaerated in a sealed vessel at a rate of at least 100 mL/min per liter of test solution until reaching the required DO level. Blank solutions were deoxygenated with nitrogen, while the test solutions were deoxygenated with carbon dioxide or a carbon dioxide: hydrogen sulfide (9:1) mixture. The test vessel containing the test specimen was separately purged with the same gas used with the solution at a rate of at least 100 mL/min for no less than one hour. The oxygen levels were detected with a HACH A1100 oxygen sensor used for process monitoring. The accuracy of the DO measurement was ± 0.1 ppb (intentionally omitted in the following discussions for the sake of simplification).

The test solutions were maintained at 24 ± 3 ºC (ambient tests) and 120 ± 3 or 140 ± 3 ºC (HTHP tests). The temperature of the HTHP tests was selected considering the usual surroundings temperature of super 13Cr tubing. The test pH values of the solution before being contacted with a test specimen were measured with a LEICI PHBJ-206 pH meter after the DO levels reached the target value. Considering the difficulties in measuring the pH under HTHP conditions, an OLI system was used for analog computation. Considering the pH value simulated at 120 ºC (1MPa of CO_2 corresponds to a pH = 3.7), the pH values of the CO_2 saturated and the blank solutions were buffered with CH_3COOH and adjusted to a constant value of 3.7. After the electrochemical tests, the specimens were further investigated by scanning electron microscopy (SEM) to check the existence of pitting phenomena.

3. RESULTS AND DISCUSSION

In order to investigate the impact of low levels of DO on the passivation properties of a super 13Cr stainless steel under CO_2/H_2S conditions, different gases (i.e., nitrogen and carbon dioxide) were used for deaeration, thereby avoiding the interference of other atmospheric gases. The polarization curves of the super 13Cr stainless steel under different DO levels are shown in Figure 2. Since some features of the passivation zone such as the length of the passivation zone and the passive current density were significantly more evident than other parameters, the corrosion resistance was observed to decrease with the concentration of DO. The corrosion (E_{corr}), pitting (E_{pit}), re-passive potentials (E_{rep}) as well as the corrosion current density (i_{corr}) derived from the curves are shown in Table 2. In the case of solutions free of CO_2 or H_2S (Figure 2a), E_{pit} and E_{rep} noticeably decreased with the concentration of DO. E_{corr} shifted to nobler values and the passive current increased with the concentration of DO in the solution, similarly to what Feng observed on.316L stainless steel [26]. In the CO_2 saturated solution, compared with Figure 2a, the E_{pit} and passive current density remained nearly unchanged under low DO levels (10–100 ppb, Figure 2b). These results were in agreement with those reported by Qiao [11] who suggested that the influence of oxygen on the anodic process decreased with the concentration of H^+. Nevertheless, we observed a significant increase in the E_{corr} at 1000 ppb of DO, thereby resulting in a poorer passivation performance. Thus, we concluded that various critical DO levels can be defined for each corrosion environment, and the relationship between the concentration of DO and the E_{corr} can be accurately obtained by strictly controlling the DO by injection other gases.

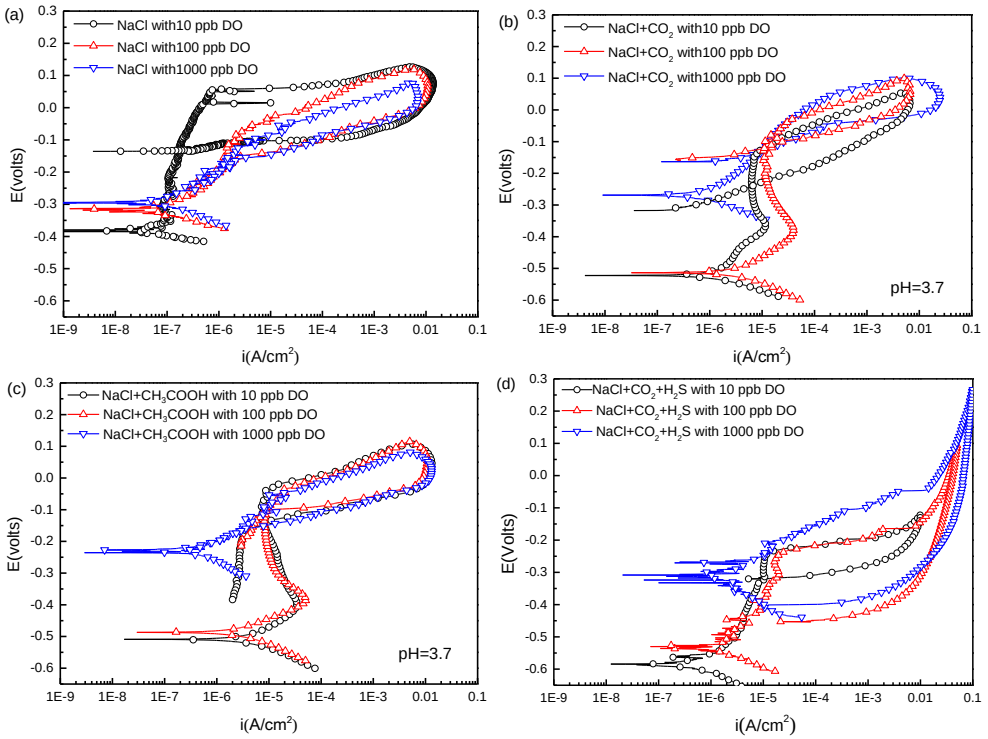

Figure 2. Potentiodynamic polarization curves for the super 13Cr steel in a 5% NaCl solution at 24 ºC: (a) saturated with nitrogen, (b) saturated with carbon dioxide (pH = 3.7), (c) saturated with nitrogen at the same pH value as in (b), and (d) saturated with a mixture of carbon dioxide and hydrogen sulfide (9:1).

Table 2. E_{corr}, E_{pit}, $E_{rep,}$ and i_{corr} values for the super 13Cr steel in a 5% NaCl solution saturated with nitrogen, carbon dioxide or a mixture of carbon dioxide and hydrogen sulfide (9:1) at 24 ºC under atmospheric pressure.

Medium	DO (ppb)	E_{corr} (mV_{SCE})	i_{corr} (A/cm^{-2})	E_{pit}	E_{rep}
NaCl + N_2	10	-0.382	2.25E-8	0.058	-0.13
NaCl + N_2	100	-0.315	3.41E-8	-0.078	-0.15
NaCl + N_2	1000	-0.298	3.41E-8	-0.122	-0.17
NaCl +CO_2	10	-0.523	1.00E-6	-0.122	-0.24
NaCl +CO_2	100	-0.491	1.20E-6	-0.100	-0.11
NaCl +CO_2	1000	-0.268	3.73E-7	-	-
NaCl +CH_3COOH + N_2	10	-0.526	3.85E-6	-0.120	-0.12
NaCl +CH_3COOH + N_2	100	-0.486	3.88E-6	-0.106	-0.13
NaCl +CH_3COOH + N_2	1000	-0.235	5.20E-7	-	-
NaCl +CO_2+H_2S	10	-0.584	7.21E-7	-0.24	-0.32
NaCl +CO_2+H_2S	100	-0.529	1.80E-6	-0.25	-0.44
NaCl +CO_2+H_2S	1000	-0.313	2.28E-6	-	-

With the aim to shed light on the reasons behind the change in the sensitive DO concentration, a blank solution buffered at pH 3.7 (Figure 2c) was used for comparison. The polarization curves at different DO levels showed the same trend with the CO_2 saturated solution, thereby indicating that the

pH (instead of the interactions between CO_2 and DO) is the main factor influencing the maximal DO level, which is in good agreement with the experimental results of Tokuri on Cu corrosion [27].

When a certain concentration of H_2S is present in the CO_2 saturated solution (Figure 2d), the overall E_{pit} at varying DO concentrations decreased. The passive current density increased upon increasing the DO concentration to 100 ppb. Furthermore, E_{corr} of the super 13Cr steel increased by 0.2 mV $_{SCE}$ when 1000 ppb of DO were present in the H_2S condition. At these conditions, active dissolution was observed.

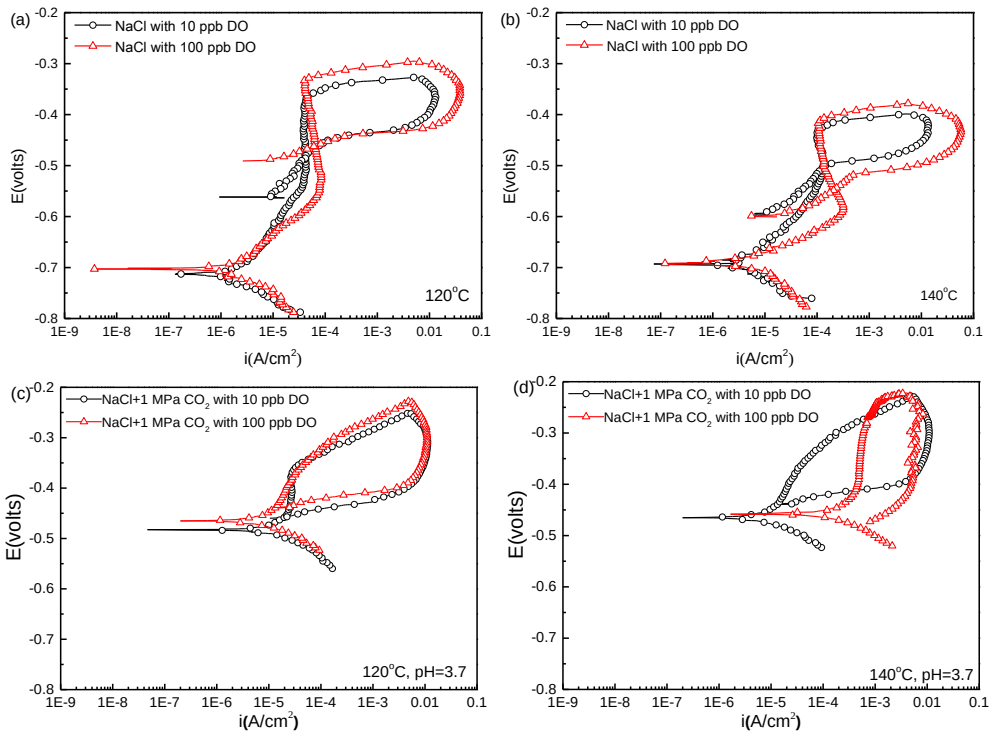

Figure 3. Potentiodynamic polarization curves for the super 13Cr steel in a 9.7% NaCl solution: (a) saturated with nitrogen at 120 ºC, (b) saturated with nitrogen at 140 ºC, (c) saturated with carbon dioxide at 120 ºC and (d) saturated with carbon dioxide at 140 ºC.

Table 3. E_{corr}, E_{pit}, E_{rep}, and i_{corr} values for the super 13Cr steel in a NaCl solution saturated with nitrogen or carbon dioxide under HTHP conditions.

Medium	DO (ppb)	E_{corr} ($mV_{Ag/AgCl}$)	i_{corr} (A/cm^{-2})	E_{pit}	E_{rep}
120ºCNaCl + N_2	10	-0.713	1.78E-6	-0.362	-0.475
120ºCNaCl + N_2	100	-0.703	2.02E-6	-0.336	-0.465
140ºCNaCl + N_2	10	-0.695	3.83E-6	-0.433	-0.505
140ºCNaCl + N_2	100	-0.695	7.88E-6	-0.415	-0.544
120ºCNaCl +CO_2	10	-0.483	1.58E-5	-0.365	-0.461
120ºCNaCl +CO_2	100	-0.466	1.68E-5	-	-
140ºCNaCl +CO_2	10	-0.464	9.65E-6	-	-
140ºCNaCl +CO_2	100	-0.459	1.81E-4	-	-

In the ambient tests, the sensitive DO concentration significantly varied depending on the conditions. Considering the practical applications of super 13Cr (i.e., formation pressure and bottom hole temperature), we decided to test the electrochemical properties of super 13Cr at 120 and 140 ºC (Figure 3). The E_{corr}, E_{pit}, E_{rep}, and i_{corr} values are summarized in Table 3.

When the solution was free of CO_2 (Figures 3 a and b), E_{corr} slightly decreased while E_{pit} moved forward to a low extent while DO increasing from 10 to 100 ppb. Nevertheless, the cyclic polarization curves at 10 and 100 ppb of DO clearly revealed different re-passivation properties at 120 or 140 ºC. A larger hysteresis loop was observed at 100 ppb of DO. In a CO_2-saturated solution at 120 ºC, 1 MPa CO_2, and pH = 3.7 (Figure 3c), the super 13Cr steel showed a noticeable passivation zone at 10 ppb of DO. However, the passivation features noticeably declined upon increasing the DO concentration to 100 ppb. When the temperature reached 140 ºC (Figure 3 d), the slope of the passive zones decreased even in the presence of 10 ppb of DO. In that case, the sensitive DO level of a super 13Cr steel at 140 ºC and 1 MPa CO_2 in 9.7 wt% NaCl was less than 10 ppb.

When no DO was present in the solution, the cathode underwent electrochemical HER:

$$2H^+ + 2e^- \Leftrightarrow H_2 \qquad (1)$$

In a solution containing DO, the cathodic process may involve a combination of HER and oxygen reduction reaction (ORR). At these conditions, the following additional cathodic reaction will be promoted upon increasing the concentration of DO in the solution, and this would have a major impact on the corrosion resistance of the stainless steel.

$$O_2 + 4H^+ + 4e^- \Leftrightarrow 2H_2O \qquad (2)$$

In general, HER is controlled by charge transfer process while ORR is a mass-controlled reaction at potentials in the more active region of super 13Cr in solutions [28,29]. Raja et al. [13] and Badea et al. [30] found out the DO promoted the stability of the passivation for stainless steel and stainless alloys in acid solutions, and believed the improvement was accelerated by the effect of DO on the cathodic process. In the contrary, Qiao et al. [11] and Feng et al. [26] found that the effect of DO were mainly consequent on the acceleration of anodic process. Based on the above, whether the DO has an impact on cathodic process still remains to be studied. We hence compare the cathodic curves under various DO levels by fitting to clarify the influence of traces of DO on cathodic process. The cathodic current density can be expressed as follows considering both the reaction (1) and (2).

$$|I_c| = I_{0,c}\exp\left(-\frac{E-E_{e,c}}{\beta_c}\right) + I_L \qquad (3)$$

Where $I_{0,c}$ is the exchange current density, $E_{e,c}$ is the equilibrium potential, β_c is the Tafel slope of HER, and I_L is the limiting diffusion current density of ORR. As shown in Fig 4, the fitting results clarify that charge transfer controlled reaction is the dominant cathodic process in all the simulative solutions even with 1000 ppb of DO. Although ORR occurred under these conditions, the amount of DO was too low to result in diffusion controlled ORR. In CO_2 statured solutions (Fig 4 b and d) or the solutions buffered with weak acid (Fig 4c), the HER is predominant cathodic process even in the presence of 1000 ppb of DO. However, it should be emphasized that the contribution of ORR to the overall cathodic process is relatively obvious in 5% NaCl saturated with N_2 (Fig 4a) because of its comparatively low hydrogen ion concentration. Still the cathodic curves under this circumstance can actually be well linearly fitted even with 1000 ppb of DO. The traces of DO promote

charge transfer processes, resulting in higher β_c. Considering the well linear relationship between $\log|I_c|$ and $E - E_{e,c}$, the real i_{corr} can be predicted by linearly extrapolating the Tafel line, which are shown in Table 2.

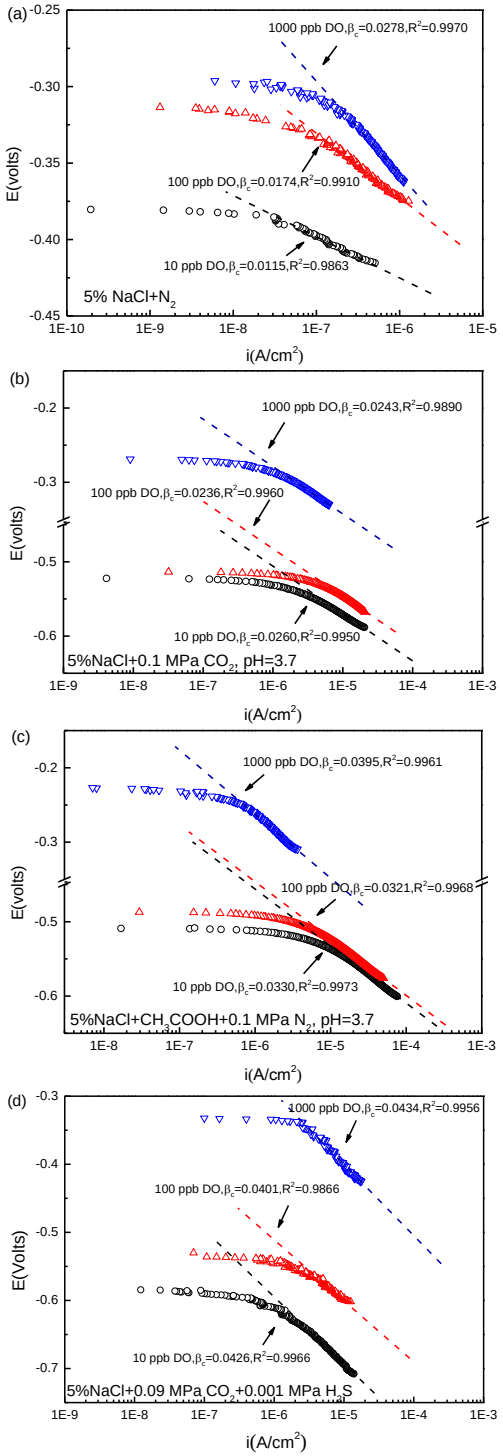

Figure 4. Cathodic fitting curves for polarization curves of super 13Cr steel in a 5% NaCl solution at 24 ºC: (a) saturated with nitrogen, (b) saturated with carbon dioxide (pH = 3.7), (c) saturated with nitrogen at the same pH value as in (b), and (d) saturated with a mixture of carbon dioxide and hydrogen sulfide (9:1).

For the HTHP environments, the contribution of ORR to the overall cathodic process weakened gradually even in 9.7% NaCl saturated with N_2 (Fig 5 a and b). The anodic processes, instead of cathodic processes, became the predominant factor affecting the corrosion resistance of super 13Cr.

In order to clarify the influence of DO on the corrosion resistance performance of the stainless steel, the ideal polarization curves were obtained (Figures 6 and 7) based on the experimental results of Figures 2 and 3. Curves A_{10} and C_{10} represent a possible ideal anodic polarization curve and a cathodic reaction at 10 ppb of DO, respectively. The A_{100} and C_{100} curves were obtained at 100 ppb of DO, while A_{1000} and C_{1000} were obtained at 1000 ppb of DO.

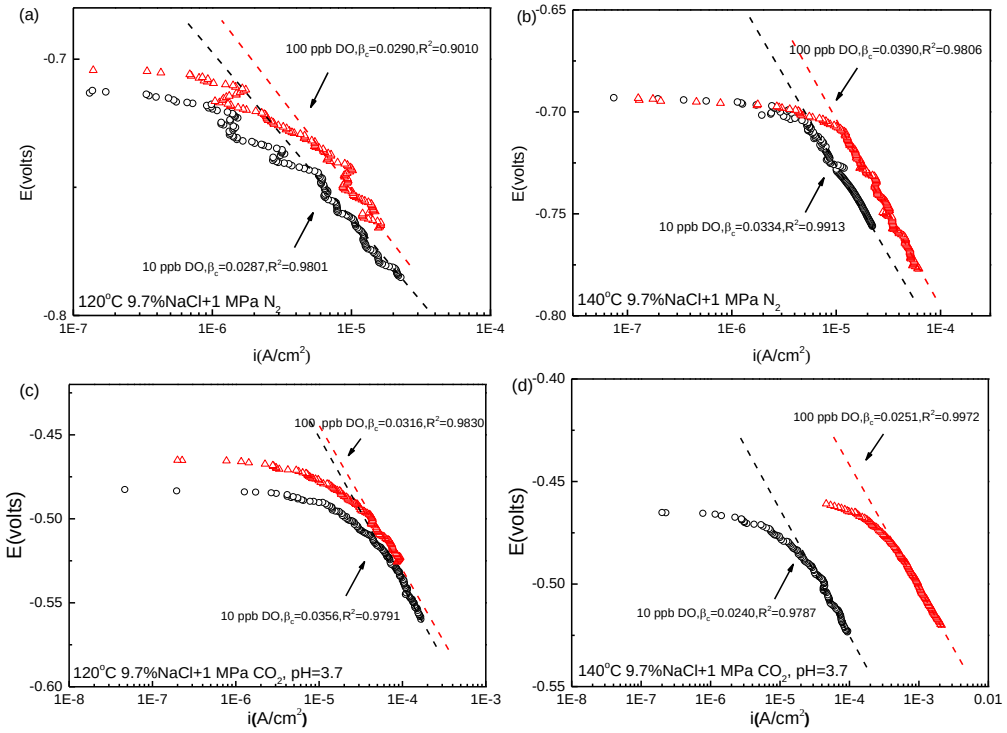

Figure 5. Cathodic fitting curves for polarization curves of super 13Cr steel in a 9.7% NaCl solution: (a) saturated with nitrogen at 120 ºC, (b) saturated with nitrogen at 140 ºC, (c) saturated with carbon dioxide at 120 ºC and (d) saturated with carbon dioxide at 140 ºC.

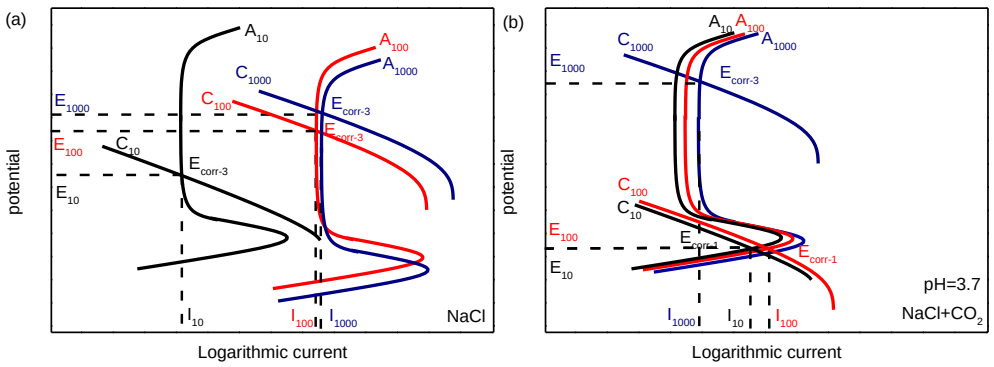

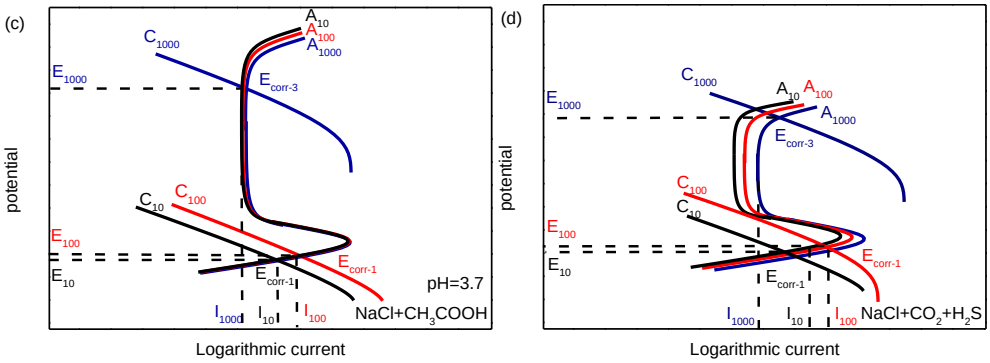

Figure 6. Ideal polarization curves for the super 13Cr steel in a 5% NaCl solution at 24 ºC: (a) saturated with nitrogen, (b) saturated with carbon dioxide, (c) saturated with nitrogen at the same pH value as in (b), and (d) saturated with a mixture of carbon dioxide and hydrogen sulfide (9:1).

At ambient temperature and pressure, a corrosion process comprised of A_{10} and C_{10} curves was assumed to intersect the steady potential (E_{corr-3}) in the blank solution (Figure 6a), which corresponded to the highest E_{corr} and lowest i_{corr} values. Although the intersections of A_{100} and C_{100}, A_{1000} and C_{1000} were located at E_{corr-3} as well, the E_{corr} became nobler while increasing i_{corr} and decreasing the passivation zone, and the corrosion resistance decreased as compared to the ideal polarization curve at 10 ppb of DO. Higher concentrations of DO favored reaction (2) and shifted the ideal cathodic polarization curve upward, while increasing the metal surface electron acceptor in the anodic reaction displaced the anodic polarization curve to the right.

In the saturated CO_2 solution (Figure 6b), the A_{10} and C_{10} as well as A_{100} and C_{100} curves of super 13Cr were assumed to intersect the active potential E_{corr-1}, which corresponded to the lowest E_{corr} and the highest i_{corr}. Compared with the blank solution, the effect of 100 ppb of DO on the passivation performance was not significant. When the DO increased to 1000 ppb, the anodic polarization approached the transpassive zone, leading to poorer passivation performances and re-passivation abilities. Additionally, the polarization process in the blank solution buffered at pH = 3.7 (Figure 6c) was similar to that in Figure 3b, thereby indicating that the passivation features of super 13Cr under different DO environments mainly depend on the pH value.

In the H_2S solution (Figure 6d), H_2S reacts with DO generating adsorbed sulfur atoms (S_{ads}) (reaction (4)) [31–33]:

$$2H_2S + O_2 \rightarrow 2S_{ads} + 2H_2O \qquad (4)$$

The effects of the H_2S compounds on the corrosion of the super 13Cr steel are generally ascribed to the influence of S_{ads} on the metal surface [34]. S_{ads} promote pitting corrosion according to the following process. First, S_{ads} may stabilize the otherwise unstable (or metastable) pits, thereby reducing the critical E_{pit}. Second, S_{ads} may preclude and hinder repassivation by sustaining active dissolution at conditions where the pit otherwise would repassivate. Third, S_{ads} may accelerate anodic dissolution owing to the catalytic nature of the accelerating effect of these species.

According to previous works, atomic sulfur adsorbed on metal surfaces is thermodynamically stable [35]. In the solution having a pH lower than 3.7, S_{ads} seemed to be stable in the -800–0 mV_{SCE} potential range. At these conditions, hydroxyl are replaced with S_{ads} atoms [36]. Therefore, at

concentrations of DO lower than 1000 ppb, S_{ads} atoms, generated by reaction between DO and hydrogen sulfide, remained stable under E_{corr} [35].

Furthermore, the remaining H_2S continuously influence the cathodic reactions by increasing the concentration of H^+ [37–39]:

$$H_2S \rightarrow H^+ + HS^- \quad (5)$$

$$HS^- \rightarrow H^+ + S^{2-} \quad (6)$$

The enhancement of the HER in the solution caused A_{10} and C_{10} to intersect the active potential $E_{corr\text{-}1}$, thereby decreasing the E_{corr} and increasing i_{corr} values of the stainless steel. When increasing the oxygen content, nobler E_{corr} were obtained and the range of passive potential slightly decreased as a result. When DO increased to 1000 ppb, A_{1000} and C_{1000} intersected the transpassive zone, thereby finally leading to the loss of the passivation ability for the super 13Cr steel.

With regard to HTHP conditions, although the effect of DO on the ideal anodic and cathodic polarization curves (Figure 7) showed similar trends as compared to ambient temperature conditions, the sensitive levels of DO varied with the temperature. In the case of a solution free of CO_2, 100 ppb of DO did not significantly alter the passivation properties of the steel. However, at 120 ºC, 1 MPa CO_2, and pH = 3.7, the cathodic and the anodic polarization curves intersected the transpassive region at a DO concentration of 100 ppb.

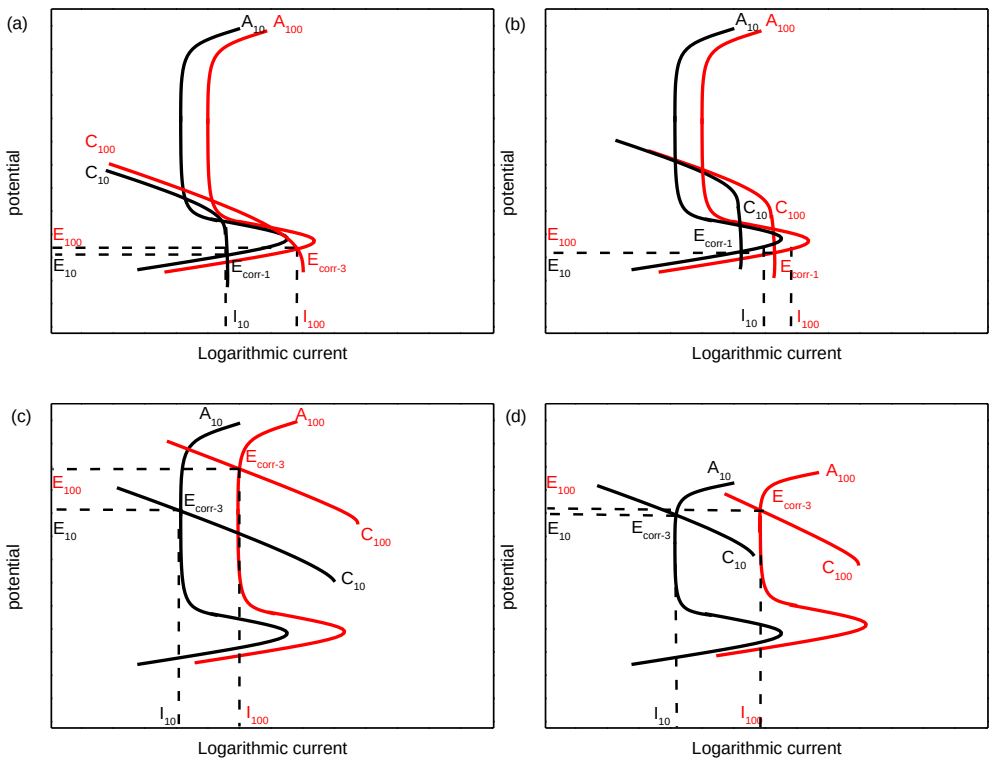

Figure 7. Ideal polarization curves for the super 13Cr steel in a 9.7% NaCl solution: (a) saturated with nitrogen at 120 ºC, (b) saturated with nitrogen at 140 ºC, (c) saturated with carbon dioxide at 120 ºC, and (d) saturated with carbon dioxide at 140 ºC.

A noticeable decrease in the passivation characteristics of the super 13Cr steel was observed under such level of DO. Moreover, the sensitive DO concentration decreased well below 10 ppb when the temperature increased to 140 ºC, and this can be produced by the relatively high E_{corr} values at a CO_2 partial pressure of 1 MPa.

At a constant temperature, the sensitive levels of DO on E_{corr} were observed to differ depending on the conditions. As shown in Figure 8, the passivation characteristics of the steel were noticeably reduced when DO increased from 100 to 1000 ppb under both CO_2 and H_2S conditions at ambient temperature. Compared with 10 ppb of DO, E_{corr} under CO_2/H_2S conditions increased to a level close to that of the blank solution at 1000 ppb DO, thereby indicating that the concentration of DO became the dominant factor controlling E_{corr}. However, the impact of DO on E_{corr} decreased with the temperature (Figures 9 a and b). This phenomenon was mainly produced by the enhancement of the cathodic reaction controlled by diffusion under HTHP conditions, which reduced the effect of traces of DO on the cathodic polarization process. Similarly, this phenomenon accelerated the transport of reaction material, thereby narrowing the gap between the electron acceptor on the metal surface under different concentrations of DO.

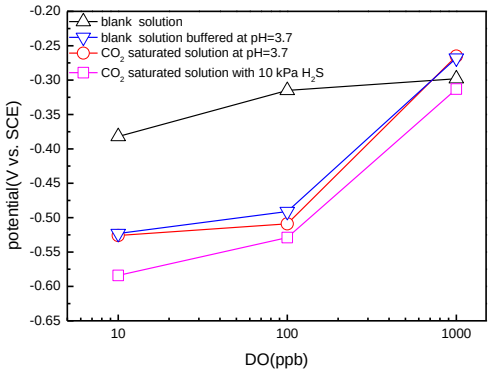

Figure 8. Corrosion potential for the super 13Cr steel as a function of the DO content in a NaCl solution at 24℃.

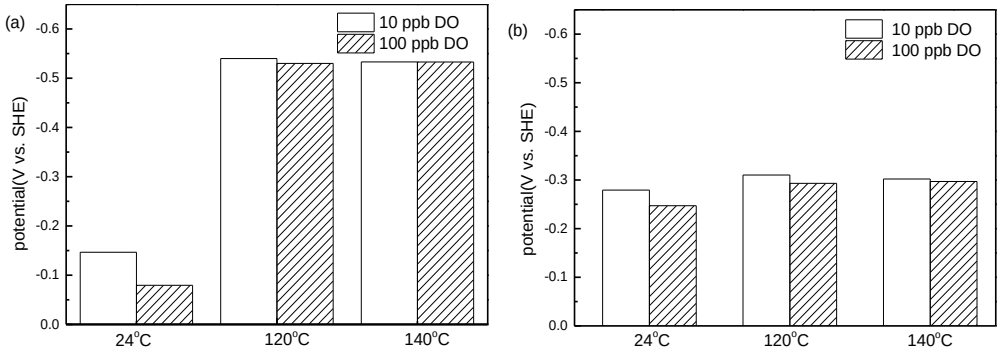

Figure 9. Corrosion potential for the super 13Cr steel at different temperatures in a NaCl solution: (b) saturated with nitrogen, (c) saturated CO_2 solution.

Additionally, DO (from 10 to 100 ppb) was found to improve the passive current density under all tested conditions (Figure 10), which demonstrates the effect of this parameter on the anode reactions. Some SEM images of the sample after the cyclic polarization tests are shown in Figure 11.

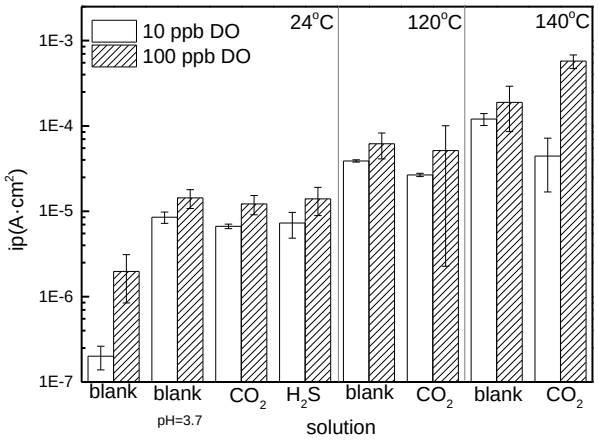

Figure 10. Passive current density for the super 13Cr steel at different concentrations of DO.

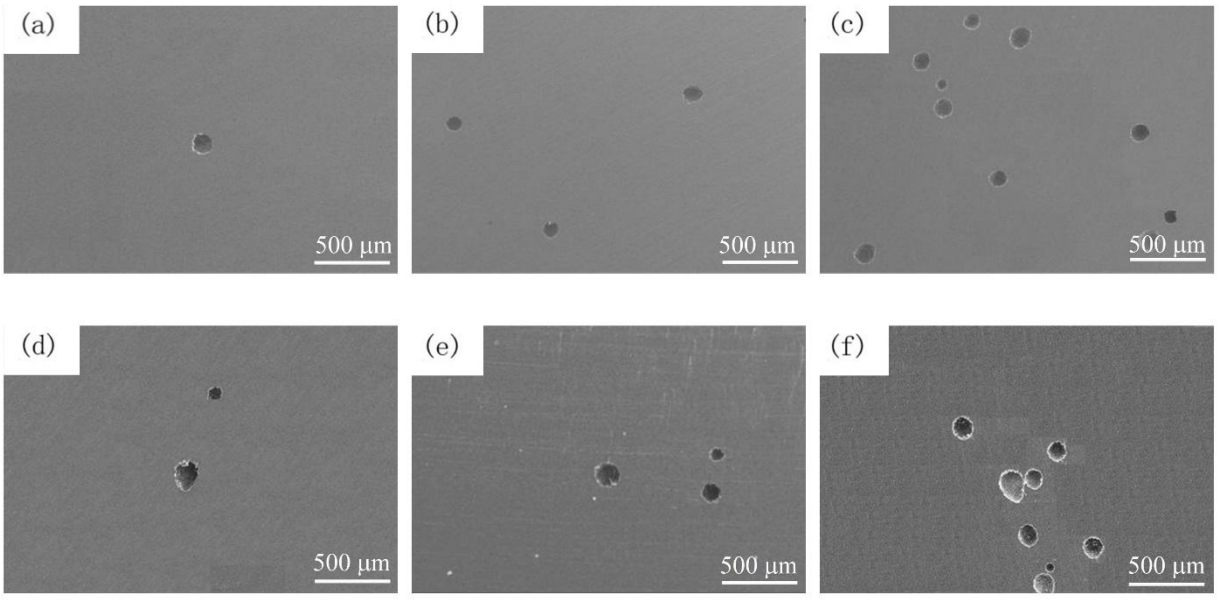

Figure 11. SEM images of the super 13Cr steel in a saturated CO_2 solution under: (a) 10 ppb, (b) 100 ppb, and (c) 1000 ppb of DO. SEM images of the super 13Cr steel in a H_2S solution under: (d) 10 ppb, (e) 100 ppb, and (f) 1000 ppb of DO.

The amount of pitting increased with the concentration of DO in CO_2 and H_2S solutions, thereby revealing that DO apparently reduced the stability of the passive film and increased the risk of localized corrosion. Under saturated CO_2 conditions, higher concentrations of DO can increase the number of available electron acceptor species on the surface of the electrode. Once reached the sensitive value, the stability and passivation characteristics of the material disappeared, as shown in

Figure 12a. Under H_2S conditions (Figure 12b), higher concentrations of DO would favor the presence of more highly surface active S_{ads} adsorbed on the metal surface [40], leading to localized corrosion even at trace amounts of DO (100 ppb).

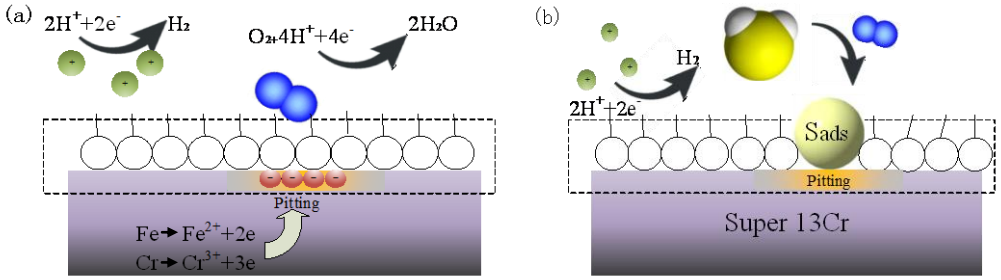

Figure 12. Schematic of the corrosion mechanism involving DO under (a) CO_2 and (b) H_2S conditions.

4. CONCLUSIONS

The passivation features of a stainless steel such as super 13Cr were significantly reduced when DO increased from 100 to 1000 ppb under both CO_2 and H_2S conditions at ambient temperature. DO became the dominant factor controlling E_{corr} at 1000 ppb of DO. However, at high temperatures, the effect of DO on E_{corr} was less pronounced, being mainly reflected in the instability of the passivation zone.

Under saturated CO_2 conditions, the effect of DO was mainly dependent on the pH value which in turns depends on the solubility of CO_2. Although 100 ppb of DO had little influence on the passivation properties of a super 13Cr steel at ambient temperature and pressure, the sensitive level of DO was lower than 100 ppb at 120 ºC and 1 MPa CO_2, and well below 10 pbb at 140 ºC.

In the presence of H_2S, the effect of this species on the corrosion resistance of a super 13Cr steel could be generally ascribed to the adsorption of S_{ads} on the passivation film. In that case, DO promoted the generation of S_{ads}, significantly decreasing the passivation and re-passivation properties of the steel at 100 ppb.

In solutions free of CO_2/H_2S, the effect of DO was mainly reflected in the reduction of the passivation stability at ambient temperature and pressure. Thus, only 10 ppb of DO could significantly reduce the slope of the passivation curve. In contrast, 100 ppb of DO had little influence on the passivation properties at high temperatures (120 and 140 ºC) and high pressure (1.5 MPa). The effect of DO was mainly reflected in the reduction of the re-passivation properties upon increasing the DO levels from 10 to 100 ppb.

ACKNOWLEDGEMENT
This work was supported by the National Natural Science Foundation of China (Grant No. 51171022 and 51371034).

References

1. V. B. Singh, A. Gupta, Active, *Mater. Chem. Phys.*, 85 (2004) 12.
2. N. Anselmo, J.E. May, N.A. Mariano, P.A.P. Nascente, S.E. Kuri, *Mater. Sci. Eng. A.*, 428 (2006) 73.
3. H. Takabe, M. Ueda, J. W. Martin, P. I. Nice, Application Limits For 110ksi Strength Grade Super 13Cr Steel In CO_2 Environments Containing Small Amounts of H_2S, *presented at NACE Annual Conference 09, NACE Corrosion/09*, Georgia, Atlanta, 2009, Paper No 083.
4. D. G. Kolman, D. K. Ford, D. P. Butt, T. O. Nelson, *Corros. Sci.*, 39 (1997) 2067.
5. Y. P. Kima, M. Fregonesea, H. Mazillea, D. Feronb, G. Santarinic, *Corros. Sci.*, 48 (2006) 3945.
6. B. Yu, D. Y. Li, A. Grondin, *Wear*, 302 (2013) 1609.
7. W. C. Baek, T. Kang, H. J. Sohn, Y. T. Kho, *Electrochim. Acta*, 46 (2001) 2321.
8. S. Wang, D. Liu, N. Du, Q Zhao, S. Liu, J. Xiao, *Int. J. Electrochem. Sci.*, 10 (2015) 4393.
9. N. D. Greene, *J. Electrochem. Soc.*, 107 (1960) 457.
10. S. H. Mameng, A. Bergquist, E. Johansson, Corrosion of Stainless Steel in Sodium Chloride Brine Solutions, *presented at NACE Annual Conference 14, NACE Corrosion/14*, Texas, San Antonio, 2014, Paper No 4077.
11. Y. X. Qiao, Y. G. Zheng, P. C. Okafor, W. Ke, *Electrochim. Acta*, 54 (2009) 2298.
12. H. Sun, X. Wu, E. H. Han, Y. Wei, *Corros. Sci.*, 59 (2012) 334.
13. K. S. Raja, D. A. Jones, *Corros. Sci.*, 48 (2006) 1623.
14. K. Ishida, D. Lister, *J. Nucl. Sci. Technol.*, 49 (2012) 1078.
15. Y. J. Kim, *Corrosion*, 51 (1995) 849.
16. Y. J. Kim, *Corrosion*, 55 (1999) 512.
17. W. Kuang, X. Wu and E. H. Han, *Corros. Sci.*, 63 (2012) 259.
18. Y. Liu, B. Zhang, Y. Zhang, L. Ma, P. Yang, *Eng. Fail. Anal.*, 60 (2016) 307.
19. T. Rogne, R. Johnsen, The effect of CO_2 and oxygen on the corrosion properties of UNS S31254 and UNS S31803 in brine solution, *presented at NACE Annual Conference 92, NACE Corrosion/92*, Texas, Houston, 1992, pp. 253-258.
20. P. Marcus, *Corrosion mechanisms in theory and practice*, Marcel Dekker, (2002) New York, USA.
21. D. Du, K. Chen, H. Lu, L. Zhang, X. Shi, X. Xu, P. L. Andresen, *Corros. Sci.*, 110 (2016) 134.
22. Y. Otsuka, S. Nagaoka, Y. Mutoh, *J. Solid Mech. Mater. Eng.*, 10 (2011) 1334.
23. J. Congleton, H.C. Shih, T. Shoji, R.N. Parkins, *Corros. Sci.*, 25 (1985) 769.
24. D. C. Smith and B. Mcenaney, *Corros. Sci.*, 19 (1979) 379.
25. *NACE MR0175 / ISO 15156*, Petroleum and natural gas industries - materials for use in H_2S-containing environments in oil and gas production, NACE International (NACE), *International Organisation for Standardisation*, 2016.
26. Z Feng, X Cheng, C Dong, X Xu, X Li, *J. Nucl. Mater.*, 407 (2010) 171.
27. K. Tokuri, Y. Yamashita, M. Shiohara, N. Oda, S. Saito, Jpn. *J. Appl. Phys.*, 49 (2010) 05FF04.
28. R. Babić, M. Metikoš-Huković, *J. Appl. Electrochem.*, 23 (1993) 352.
29. D. Sidorin, D. Pletcher, B. Hedges, *Electrochim. Acta*, 50 (2005) 4109.
30. G. Badea, D. Ionita, P. Cret, *Mater. Corros.*, 65 (2014) 1103.
31. S. B. Maldonadozagal and P. J. Boden, *Br. Corros. J.*, 17 (1982) 116.
32. E. Körös, L. Maros, I. Fehér, E, Schulek, *J. Inorg. Nucl. Chem.*, 4 (1957) 185.
33. A. Ikeda, M. Igarashi, M. Ueda, Y. Okada, H. Tsuge, *Corrosion*, 45 (1989) 838.
34. J. Enerhaug, Ø. Grong, U. Steinsmo, *Sci. Technol. Weld. Joi.*, 6 (2001) 330.
35. P. Marcus: Sulfur-Assisted Corrosion Mechanisms and the Role of Alloyed Elements. ("Corrosion Mechanisms in Theory and Practice", P. Marcus and J. Oudar eds.). *Marcus Dekker*, 1995, pp. 239-263.
36. P. Marcus, E. Protopopoff, *J. Electrochem. Soc.*, 137 (1990) 2709.

37. X. Cheng, H. Ma, G. Li, S. Chen, Z. Quan, S. Zhao, L. Niu, *Corros. Sci.*, 42 (2000) 299.
38. X. Cheng, H. Ma, S. Chen, L. Niu, S. Lei, R. Yu, Z. Yao, *Corros. Sci.*, 41 (1999) 773.
39. H. Ma, X. Cheng, S. Chen, C. Wang, J. Zhang, H. Yang, *J. Electroanal. Chem.*, 451 (1998) 11.
40. R. H. Jones, D. R. Baer, C. F. Windisch, R. B. Rebak, Corrosion Enhanced Enrichment of Sulfur and Implications for Alloy 22, *presented at NACE Annual Conference 06, NACE Corrosion/06*, Texas, Houston, 2006, Paper No 621.